Microfluid Nanofluid (2011) 10:1289–1298
DOI 10.1007/s10404-010-0760-7

ORIGINAL PAPER

A modified microfluidic chip for fabrication of paclitaxel-loaded poly(L-lactic acid) microspheres

Tianxi He · Qionglin Liang · Kai Zhang · Xuan Mu · Tingting Luo · Yiming Wang · Guoan Luo

Received: 20 October 2010 / Accepted: 16 December 2010 / Published online: 11 January 2011

Abstract In this article, we present a simple PDMS surface modification method based on poly(vinyl alcohol)/glycerol (PVA/Gly) solution immersion, self-assembled absorption, and heat treatment. The results of contact angle and ATR-FTIR demonstrate the superhydrophilic surface in modified PDMS. It can allow for the stable production of monodisperse droplet in a highly reproducible manner. In addition, we demonstrate the fabrication of monodisperse paclitaxel (PTX) loaded poly(L-lactic acid) (PLLA) microspheres on this kind of modification chip with solvent evaporation. The PLLA microspheres can be adjusted to a range of different sizes depending on the system flow rate. Determination of microsphere size is carried out by optical microscopy and image analysis to reveal less than 4% variation in microsphere size. Compared with the results of published papers, the presented data demonstrate that PTX-loaded PLLA microspheres show good physical properties (spherical and discrete), high-drug loading, encapsulation efficiency, a small initial burst, and sustained-release behavior due to outstanding monodispersity. With the characteristic to prepare high-quality, monodisperse, biodegradable microspheres, the versatile and simple microfluidic method facilitates the development of more reliable and reproducible drug delivery systems, which have great potential to benefit pharmaceutical and biological applications.

Keywords Microfluidic · Droplets · Poly(L-lactic acid) microsphere · Paclitaxel · Drug delivery · Monodisperse

1 Introduction

Effective drug delivery systems (DDSs) are required for the drug to reach the target site and maintain sufficient therapeutic activity. Successful DDSs need not only optimal drug loading capacity and release properties, but also good biocompatibility and low toxicity (Barratt 2003). Several DDSs, such as biocompatible polymeric microsphere (BPM) and microcapsule (Freiberg and Zhu 2004; Park et al. 2007; Oh et al. 2008), liposome (Lim et al. 2008), polymeric micelle (Wei et al. 2009) and others (Kim and Dobson 2009), have been successfully prepared. BPM has been explored extensively as DDS because of their ease of delivery and the ability to regulate their drug release kinetics (Freiberg and Zhu 2004; Park et al. 2007). Conventional BPM production techniques, however, create BPM with broad distributions in size because of the inhomogeneous forces involved, therefore cause size, morphology, and quality discrepancy within different batches, and bring about unpredictable in the degradation rate of BPM and the kinetics of drug release (Freiberg and Zhu 2004), which limiting its clinical application (Little et al.

Electronic supplementary material The online version of this article (doi:10.1007/s10404-010-0760-7) contains supplementary material, which is available to authorized users.

T. He · Q. Liang (✉) · Y. Wang · G. Luo (✉)
Key Laboratory of Bioorganic Phosphorus Chemistry & Chemical Biology (Ministry of Education), Department of Chemistry, Tsinghua University, Beijing 100084, People's Republic of China
e-mail: liangql@tsinghua.edu.cn

G. Luo
e-mail: luoga@tsinghua.edu.cn

T. He
Logistic Engineering of University, Chongqing 400016, People's Republic of China

K. Zhang · X. Mu · T. Luo
School of Pharmacy, East China University of Science and Technology, Shanghai 200237, People's Republic of China

2004; Lassalle and Ferreira 2007; Oh et al. 2008; Marre and Jensen 2010).

Monodisperse BPM has been shown to be important in controlling drug release kinetics, reproducibility, and bioavailability (Wang et al. 2005; Xu et al. 2009). To date, various methods have been proposed to prepare monodisperse BPM (Lassalle and Ferreira 2007; Oh et al. 2008). Recently, droplet microfluidic method has been proven useful in the generation of monodisperse droplets (Teh et al. 2008; Zhang et al. 2009). Taking advantage of the periodic and predictable breakup of immiscible fluids, discrete and consistently sized droplets can be formed in a T-junction channel and a flow-focusing (Teh et al. 2008). By using droplet microfluidics, several groups have prepared monodisperse BPM (Kim et al. 2007; Tan and Takeuchi 2007; Dendukuri and Doyle 2009; Xu et al. 2005, 2009; Oh et al. 2008; Huang et al. 2008; Yeh and Lin 2009; Hung et al. 2010). Several monodisperse BPM of mixed drug have been successfully fabricated by droplet microfluidics, including poly(D, L-lactide-co-glycolide) (PLGA) (Xu et al. 2009), alginate (Zhao et al. 2009), chitosan (Gong et al. 2009), and others (Huang et al. 2009; Shum et al. 2008; Nisisako et al. 2006).

Paclitaxel (PTX), as a major taxoids anticancer drug, is commonly used in treatment of a variety of cancers, including lung, breast, and ovarian cancer (Spencer and Faulds 1994). Due to limited bioavailability, poor solubility, low-therapeutic index, and high-systemic toxicity, its utility in clinical treatment is restricted in many cases (Szebeni et al. 1998). By mean of DDS, these problems can be improved and addressed (Skwarczynski et al. 2006). Polylactic acid (PLA), a carrier material of approved by the US Food and Drug Administration, is commonly used as protein and DDSs owing to its biocompatibility and biodegradability (Lassalle and Ferreira 2007). There have been many reports in preparing PTX-loaded PLA microspheres using conventional methods (Liggins et al. 2000; Liggins and Burt 2001, 2004; Kang et al. 2008; Lu et al. 2008; Lee et al. 2008; Song et al. 2010). Whereas the microspheres size distribution of these reports is generally very broad. Small-sized and monodisperse PLA microspheres are especially desired to optimize their efficiency when being used for DDSs (Lassalle and Ferreira 2007). Droplet microfluidic have successfully prepared liquid core or hollow PLA microcapsules and PLA microspheres (Lensen et al. 2010; Zhu et al. 2010). However, these published approaches did not investigate their respective drug release behavior and these particles have broad size distributions. Glass chip and manual assembly of nozzles (or capillary tubes) fabrication process is very complex and time consuming. In addition, there are no reports regarding preparation of PTX-loaded BPM using microfluidic approach and evaluation of release properties of these monodisperse drug-loaded microspheres.

Here, we report on a surface modification microfluidic approach to fabricate monodisperse PTX-loaded PLLA microspheres. Our study focus on three novel features: (a) a simple surface modification method yielding superhydrophilic PDMS microchannels; (b) the production of satisfactory PTX-loaded PLLA microspheres in terms of perfect spherical shape, narrow size distribution, and high encapsulation efficiency (EE); and (c) investigation of the mechanisms and kinetics of PTX released from monodisperse PLLA microspheres.

2 Materials and methods

2.1 Materials

PTX was purchased from National Institute for the Control of Pharmaceutical and Biological Products (Beijing, China). Poly(L-lactic acid) (PLLA, $M_w = 10000$, Sigma) was used as the material for microspheres. Poly(dimethylsiloxane) (PDMS; Sylgard 184) was obtained from Dow Corning (Midland, USA). HPLC-grade acetonitrile (ACN) was purchased from Fisher Scientific (Fair Lawn, USA). Poly(vinyl alcohol) 1750 ± 50 (PVA), dichloromethane (DCM), glycerol (Gly), and 0.1 mol/L phosphate-buffered saline (PBS, pH 7.4) solutions were obtained from Sinopharm Chemical Reagent Co. Ltd (Beijing, China). Purified water used throughout the experiments was generated from Milli-Q water purification system (Millipore, Bedford, USA). All other reagents were of analytical grade and used as received.

2.2 Surface modification of microfluidic chip

Microfluidic chip with typical channel dimensions of 100 μm in depth and 200 μm in width was fabricated by conventional soft lithography techniques (Xia and Whitesides 1998). The width of flow-focusing point of the chip was decreased to 100 μm. The microfluidic chip was molded by a mixture of PDMS elastomer base/curing agent in 10:1 ratio from SU-8 mold and bonded to a flat PDMS substrate under plasma treatment for 90 s (Harrick Plasma Cleaner PDC-32G, USA). Since this is an oil-in-water (O/W) droplet generation process and there is a favorable wettability between DCM and PDMS, surface treatment is applied to the channels to make the PDMS surface hydrophilic. Plasma-treated chip was immediately filled with a 2% PVA–5% (wt%) Gly (PVA/Gly) aqueous solution and then placed at room temperature for 20 min. After that the channels were emptied by a vacuum pump and PDMS chip was put in 60°C oven for 2 h to dry and immobilize the PVA and Gly. The above procedure was repeated once, resulting in two layer coating. Finally, the

coating was thermally immobilized in an oven at 100°C for 20 min. After that the chip was allowed to cool down to room temperature inside the oven. For contact angles (CA), atomic force microscopy (AFM) images and attenuated total reflection-Fourier transform infrared (ATR-FTIR) measurement, the upper face of the plasma treatment PDMS plate was, respectively, immersed in 2% PVA, 5% Gly, and PVA/Gly solution for 20 min, and other procedure was the same as that in coating PDMS channels. The measurements of water CA were carried out on a Dataphysics OCA12 optical contact angle system at room temperature. Each data point given was based on three CA measurements at three different positions on the PDMS specimen. Static CAs were measured following the method previously reported (Lam et al. 2001). Surface morphology (AFM images) of PDMS specimens was acquired in tapping mode with a commercial multimode Nanoscope IV from Veeco in air (Santa Barbara, CA). Silicon probes (Veeco Probes, Camarillo, CA) were used with a nominal scanning rate of 0.5984 Hz. The ATR-FTIR spectra of unmodified and modified PDMS substrates (2 cm × 1 cm) were performed using a Bruker IFS 66/S spectrometer in the range 4000–500 cm^{-1} with a resolution of 4 cm^{-1}. The critical incident angle $\theta = 45°$ was used in this work.

2.3 Fabrication of monodisperse droplets and PLLA microspheres

The PTX-loaded PLLA microspheres were prepared in the microfluidic chip following the sequential three steps (Fig. 1a): (1) generation of O/W droplets, (2) collection of monodisperse droplets, and (3) PLLA microsphere preparation by solvent evaporation. The dispersed phase flowing through inlet 1 comprised 40 mg/ml PLLA and 2 (or 1) mg/ml PTX in DCM, that is, the drug-to-PLLA ratio were taken as 1/20 or 1/40, corresponding to the theoretical loading (TL) of 4.76 or 2.44%. The continuous phase flowing through inlets 2 and 3 was an aqueous solution of 2% PVA. All the solutions were loaded into syringe and connected microfluidic chip by Teflon tubing (1.6 mm OD, 0.6 mm ID). At the end of outlet, the tubing was immersed into a 10-ml beaker containing 1.0% PVA solution (40°C) to collect monodisperse droplets. Then the solvent was removed from the droplets before formation of the microspheres. We used three syringe pumps (Harvard Apparatus, model 11 plus, USA) to deliver and control the flow rates into inlets 1 (Q_1), 2, and 3 ($Q_2 = Q_3$). The flow rate range of Q_1 was from 0.03 to 0.80 ml/h, and Q_2 and Q_3 from 0.10 to 0.45 ml/h for obtaining the PLLA droplets and microspheres of different sizes. Microspheres were filtered and washed three times with purified water. At last, all the microspheres were dried at 37°C in vacuum.

We prepared four PTX-loaded PLLA microspheres with different sizes and TL. The four microspheres samples were defined as S1-1, S1-2, S2-1, and S2-2 in terms of sizes and TL (as shown in Table 1).

2.4 Characterization of droplet and microsphere size

Droplet formation was monitored under an inverted optical microscope coupled to a charge coupled device (CCD) (Daheng, China). Microscopic photographs of the collected droplets and microspheres were obtained with a CCD camera (DP 6.3.0.5, Olympus) mounted on an inverted microscope (IX71, Olympus). A hundred droplets or microspheres were randomly selected from the IX71 optical microscopy, and the sizes were measured by hand.

2.5 Drug loading, encapsulation efficiency, and in vitro drug release study

The analyses of PTX in vitro were performed by RP-HPLC (Agilent LC 1100) with a Kromasil RP-18 column (250 × 4.6 mm). A mobile phase of ACN/water (1:1 v/v) was used at a flow rate of 1.0 ml/min. Sample solution was injected at a volume of 20 µl and determined by UV absorption at 227 nm. The absorption values were converted into concentration of PTX using a standard curve generated from solutions with known concentration of the drug. Actual drug loading (AL) and encapsulation efficiency (EE) for PTX-loaded PLLA microspheres were determined by dissolving dried PTX-loaded microspheres

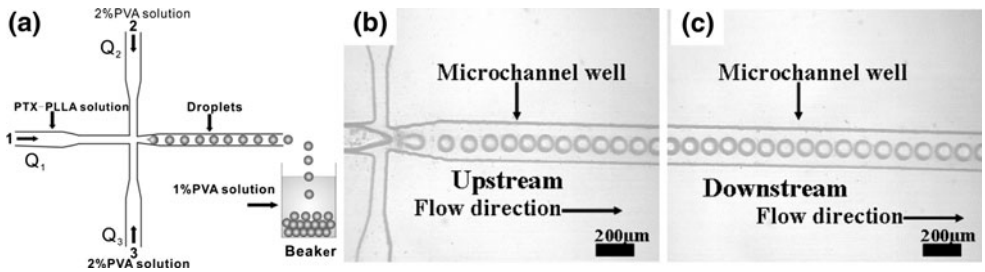

Fig. 1 **a** Schematic diagram of the microfluidic chip used for synthesis of PLLA microspheres. Optical microscopy images showing **b** the flow-focusing region generating droplets and **c** monodisperse droplets downstream. Condition: $Q_1 = 0.20$ ml/h; $Q_2 = Q_3 = 0.15$ ml/h

Table 1 Formulation parameters and characteristics of the studied PTX-loading PLLA microspheres

Sample name	S1-1	S1-2	S2-1	S2-2
D (μm)	30.80 ± 1.16	31.25 ± 1.24	49.35 ± 1.41	49.67 ± 1.59
CV (%)	3.75	3.96	2.85	3.20
TL (%w/w)	2.44	4.76	2.44	4.76
AL (%w/w)	2.36 ± 0.05	4.64 ± 0.11	2.39 ± 0.02	4.73 ± 0.07
EE (%)	95.72 ± 2.05	96.48 ± 2.31	93.95 ± 0.82	95.37 ± 1.47
R	0.973	0.939	0.967	0.974

D the average microsphere size, $D = \sum Di/n$; CV the variation coefficients of microsphere size, $\mathrm{CV} = \left[\sum (Di - D)^2/n\right]^{1/2}/D$ (D and CV based on 100 microspheres counted by hand); TL the theoretical loading; AL actual loading; EE encapsulation efficiency; R is correction coefficients of Higuchi's model

in DCM. Specifically, 1 mg microspheres were dissolved first in 1 ml DCM and underwent sonication for 2 min, to which 2 ml of mobile phase was added, and vortexed for 2 min. Then the mixture was allowed to phase separate for 15 min. A nitrogen stream was introduced to volatilize the DCM at 40°C. Subsequently, mobile phase was added to the solution to a fixed volume of 2 ml and was treated by ultrasound for 5 min and centrifuged at 4000 rpm for 10 min, obtaining a clear extracted solution for HPLC analysis. Experiments with spiked samples showed that the extraction recovery of PTX was 88.8% using this method. Each experiment was carried out in triplicate. The differences of determination AL and EE is that it has a drying process after repeat washing before determination the EE. The AL and EE of drug were defined as: $\mathrm{AL} = (W_1/W_2) \times 100\%$; $\mathrm{EE} = (W_3/W_4) \times 100\%$, where W_1 is the weight of drug recovered in PLLA microspheres, W_2 is the total weight of the drug and PLLA microspheres, W_3 is the weight of the drug recovered in PLLA microspheres with water washing for many times, and W_4 is the total weight of PTX used in the process.

In order to study in vitro PTX release, 5 mg of PTX-loaded PLLA microspheres was dispersed into 10 ml PBS at 37°C with the shaking at 100 rpm. At appropriate time intervals, the solution was centrifuged at 2000 rpm for 5 min, and 2 ml of the supernatant was collected and replaced with an equal volume of fresh PBS. Five milliliter of DCM was added to collected supernatant and the mixture shaken for 5 min to facilitate PTX extraction. After 15 min of allowing the DCM and aqueous to phase separate, the aqueous supernatant was removed by pipette. Subsequently, DCM was removed by a nitrogen stream, and 1 ml ACN was added and vortexed for 2 min. The concentration of PTX in samples was analyzed by HPLC as described above. Three known concentration of PTX standard solutions were treated under the same conditions and the mean extraction efficiency was 84.0%. Each experiment was carried out in triplicate.

The simple exponential relation $M_t/M_o = Kt^n$ is introduced to describe the general solute release behavior of controlled release polymeric system, where M_t and M_o are the cumulative mass of the diffusing compound released from the PLLA microspheres after t and infinite time (o), respectively, t is the release time, K is a constant, and n is the diffusion exponent characteristic of the release mechanism (Ritger and Peppas 1987). For linear fit, $M_t/M_o = Kt^n$ is modified to Eq. 1. In this case, n is obtained from the slope of the plot of log (M_t/M_o) versus log t

$$\log(M_t/M_o) = \log\ K + n \log\ t. \quad (1)$$

3 Results and discussion

3.1 Hydrophilic modification

In spite of its easy fabrication, elastomeric, optically transparent, and biocompatible, the strong hydrophobicity of PDMS surface makes it difficult to fill microchannels with aqueous solutions without any surface processing (Whitesides 2006; Mora et al. 2007). The surface of PDMS can be made hydrophilic using a simple air (or oxygen) plasma treatment; however, this property is quickly lost through hydrophobic recovery after exposure to air (Kim et al. 2001). Unlike previous report (Xu et al. 2009), we found that dispersed phase would attach to the channel surfaces because of its higher wettability on hydrophobic PDMS surfaces, which results in the distortion of flow pattern and eventually the failure of droplets generation immediately and continuously (Supplementary Fig. 1). To eliminate the undesired surface attachment, the surface properties of PDMS are often required to be modified into hydrophilic (Wong and Ho 2009; Zhou et al. 2010). Wu et al. (2005) modified PDMS surface with multilayer of PVA by using thermal immobilization to suppress protein adsorption and EOF, and observed good separation of basic

proteins. Kozlov et al. (2003) found that PVA adsorbed irreversibly from aqueous solutions onto hydrophobic solids in contact with solutions. Here, we develop a modified method of PDMS surface using PVA/Gly for obtaining hydrophilic properties and stable O/W droplets. PVA/Gly can be adsorbed on air plasma-treated PDMS, since the resulting surface possesses a highly hydrophilic layer with hydroxyls, silanols, and carboxylic acids, and then heat immobilized. The surface wettabilities of the PDMS plates before the plasma treatment and after the plasma treatment were investigated by water CAs. The water CA of native PDMS was 119.8 ± 0° (Fig. 2a), exhibiting hydrophobicity. Although its wettability can be increased by air-plasma exposure (CA < 45°), however, this hydrophilic property induced by plasma treatment could be only last a very short time. In our experiments, 8 h after the plasma-treated, the surface of native PDMS has gradually returned to its original hydrophobic property, and the water CA of PDMS was reduced to 83.9 ± 0.5° (Fig. 2b). For comparison, the surfaces of plasma treatment PDMS were modified with PVA and PVA/Gly, respectively, as described in Sect. 2.2. The water CA was also measured 8 h later after all modification. After PVA modification, the water CA was decreased from 119.8 ± 0° to 60.1 ± 1.0° (Fig. 2c) and indicated that the surface of the PVA-coated PDMS was hydrophilic. When the surface of plasma treatment PDMS was modified with PVA/Gly, the water CA was reduced to 35.2 ± 0° (Fig. 2d), indicating that the surface became more hydrophilic. After two cycles PVA modification, the water CA of PDMS was decreased from 119.8 ± 0° to 50.5 ± 1.2° (Fig. 2e), which indicates the surface of PDMS becomes high hydrophilicity. When the PDMS surface was modified with PVA/Gly within two cycles, the water CA of PDMS was dramatically reduced to 6.0 ± 0° (Fig. 2f), indicating that the surface took on superhydrophilic properties. Moreover, aging effect of the PVA/Gly-modified PDMS surface, 90 days storage in air, has little impact on its water CA (CA = 20.3 ± 0°), which is found to be still much lower than that of other modified groups. These experimental results demonstrated that the hydrophilic properties of two-treatment PDMS with PVA/Gly were much better than that of other modified groups. Therefore, two-layer PVA/Gly-coated PDMS was chosen for the studies.

AFM images of were performed on native PDMS, PVA-modified PDMS, and PVA/Gly-modified PDMS to observe changes in surface morphology as a result of the surface treatment (see the Supplementary Fig. 2). Native PDMS exhibits flat and uniform surfaces. In contrast, PVA-modified and PVA/Gly-modified PDMS exhibit a rugged surface with some protuberances, which result from the formation of PVA and PVA/Gly layers bonded to the surface. Compared with PVA-modified PDMS, the protuberances of PVA/Gly-modified PDMS surface are relatively evenly distributed due to highly disordered and less capable of ordering or crystallizing after adding Gly (Liang et al. 2009). Figure 3 shows the ATR-FTIR spectra of the native, two Gly treated, two PVA treated, one PVA/Gly, and two PVA/Gly treated PDMS surfaces. In the ATR-FTIR spectrum of the native PDMS, there was no infrared absorption between 3030 and 4000 cm^{-1}, while in the spectra of the PVA or Gly-treated PDMS a broadened band

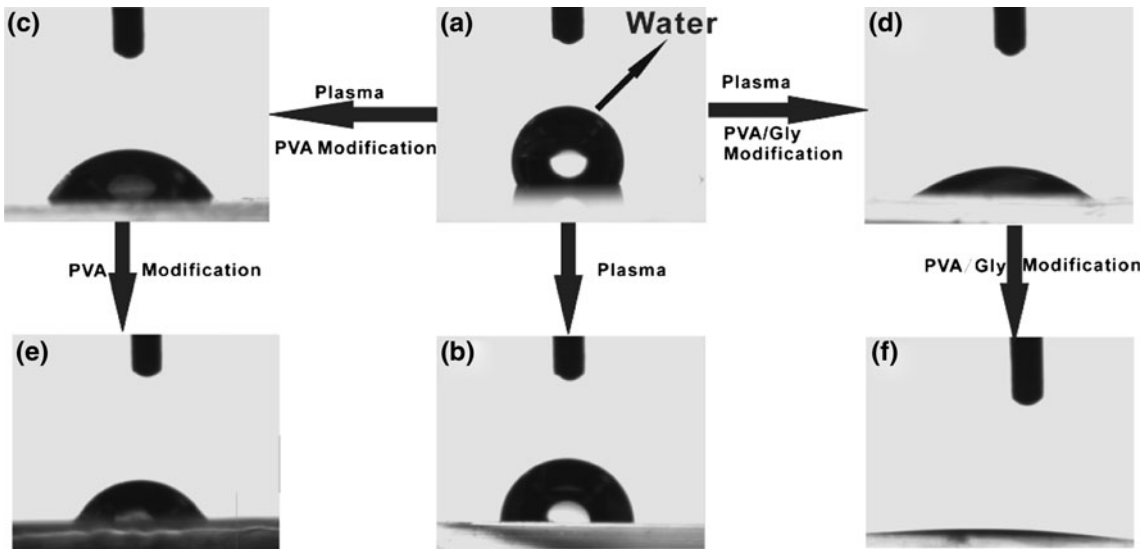

Fig. 2 Water contact angles measure **a** native PDMS plate; **b** after plasma treatment; **c** after further treatment with 2% PVA solution; **d** after further treatment with 2% PVA–5% Gly solution; **e** after further treatment with 2% PVA solution twice; **f** after further treatment with 2% PVA–5% Gly solution twice. All performed 8 h after treatment

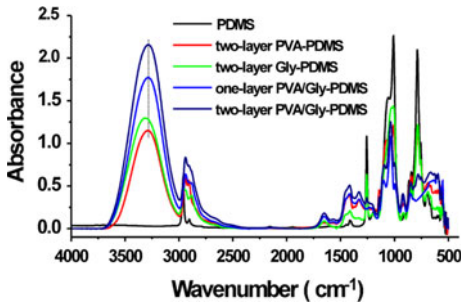

Fig. 3 ATR-FTIR spectra of native PDMS, plasma-treated PDMS coated with two-layer PVA, plasma-treated PDMS coated with two-layer Gly, plasma-treated PDMS coated with one-layer PVA/Gly, and plasma-treated PDMS coated with two-layer PVA/Gly. The spectra clearly reveal the presence of the O–H stretch and peak absorption values of the O–H stretch are different with different modified methods

at ca. 3395 cm^{-1} was observed, which was attributed to –OH stretch vibration of PVA or Gly. The dominant group $–OSi(–CH_3)_2O–$ has no infrared absorption in the range of 3100–3700 cm^{-1}, indicating that PVA or Gly has been successfully coated on the PDMS surface. As compared to that of Gly–PDMS and PVA–PDMS, strong increase in the peak density around 3100–3600 cm^{-1} occurred due to the increase of –OH concentration in PVA/Gly–PDMS with the introduction of glycerol. Compared with the ATR-FTIR spectrum of PDMS surface with PVA/Gly treated once, that of treated twice cause the intensity of –OH absorption peak increase. This result indicates that repeated treatments are in favor of increasing the wettability of PDMS surface. Moreover, the center of the –OH stretching band in PVA/Gly–PDMS shows a red shift, which implies that the addition of Gly resulted in a new hydrogen bonding environment of the system (Liang et al. 2009). The probable reaction mechanism for the attachment of PVA/Gly to the plasma oxidation of PDMS surfaces is shown in Supplementary Fig. 3. The probable mechanism of PVA/Gly assembly on the PDMS surface can be explained by the three following aspects: (1) Gly is a critical bridge and tie in building the relationship between PVA and PDMS, strengthening the interactions of them for decreasing the steric hindrance of PVA molecular. (2) Gly can readily bind to the –OH of PDMS surface and PVA due to its high hydrophilic properties. The –OH of Gly act with molecular chains of PDMS surface, preventing hydrophobic siloxane groups formation in PDMS surface (Suyatma et al. 2005). Similarly, the -OH can act with PVA molecules to reduce intramolecular interaction of PVA. (3) Gly can decrease the crystalline level of PVA, which would lead to more hydrophilic PDMS surface. Thus, improvement of the self-assembling behavior of PVA by this method can improve hydrophilicity of the microchannel surface. The specific mechanism of PVA/Gly modification of PDMS surface deserves further investigation.

3.2 Formation of monodisperse droplets

The PVA concentration has effect on the generation of droplets. The experiment indicated that it was hard to generate stable and monodisperse droplets when the concentration of PVA less than 0.5%, and the collected droplets fuse together when the concentration of PVA less than 1.5%. Therefore, 2% PVA was choice as the optimal condition to stabilize and inhibit coalescence of the droplets. Upon this modified surface, stable O/W droplets can be generated. As shown in Fig. 1b, the PLLA solution was sheared by the continuous phase to generate monodisperse droplets at the flow-focusing region (please refer to Supplementary video). During the continuous usage and observation in 7 days, the stable formation of uniform droplets indicated that the hydrophilic surface modified was stabled and was able to last for a long time. The CA of modified PDMS plates after 7 days of continuous flushing with 2% PVA was 40.4 ± 0.3° and further demonstrated that PVA/Gly treated the PDMS surface was stable for a long time. The droplets travelled through the microchannel without difficulty or wetting the walls (Fig. 1c). The heat treatment enhanced the adhesion strength of PVA/Gly to the PDMS surface and PVA/Gly layer rejected hydrophobic groups to move to the surface, which improved the stability of the modification and enables for superhydrophilic surface. Figure 4a–c showed the micrographs of droplets assembled at the cover slides. The generated droplets were well monodisperse at three different flows, and the variation coefficients were less than 1.5%.

Supplementary Fig. 4 showed the relationships between the droplet size and the flow rates of dispersed phase and continuous phase. Under a dynamic balance, the relationship $Q_d = V_d f_d$ holds, where Q_d is the flux of the dispersed phase, V_d is the volume of the droplets, and f_d is the break-up rate of the disperse phase (Nisisako et al. 2006; Zhao et al. 2009). For example, to prepare smaller droplets, we increased the continuous phase, Q_c, while fixed the flux of the Q_d. The shear force on the tip of the dispersed phase flow subsequently increased, which leaded to a decrease in the value of V_d (Zhao et al. 2009). Similarly, as the Q_d decreased while fixed the flux of Q_c, the value of V_d decreased. For a given 0.15 ml/h of the continuous phase flow rate, the droplet size decreased as the flow rate of the dispersed phase decreased. For a given 0.25 ml/h of the dispersed phase flow rate, the droplet size decreased as the flow rate of the continuous phase increased.

3.3 Formation of monodisperse PTX-loaded PLLA microspheres

With the DCM evaporation, the concentration of PLLA solution progressively increased and initiated crosslink

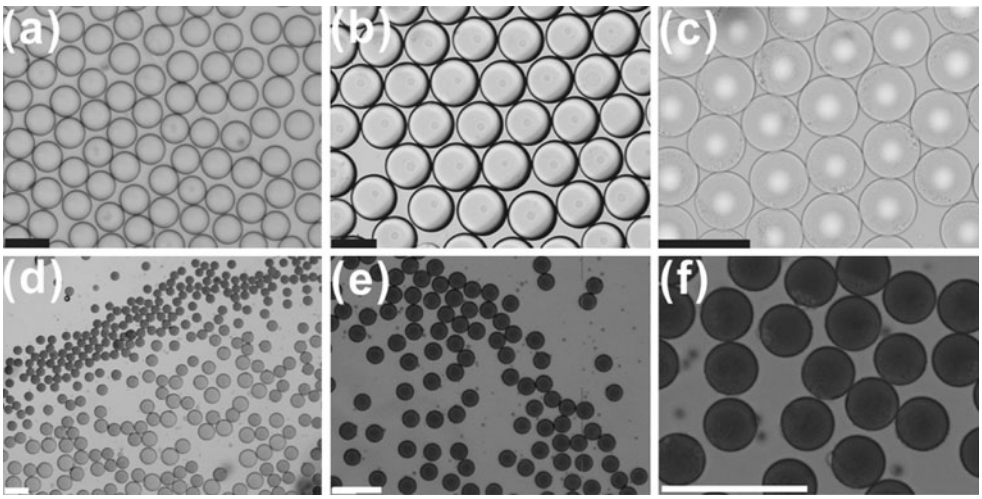

Fig. 4 Optical micrographs of **a–c** PLLA droplets assembled in cover slides; **d** PLLA droplets shrink to form solidified PLLA microspheres at the reservoir and **e–f** magnified monochrome micrographs of solidified microspheres. Conditions: **a** $Q_1 = 0.15$ ml/h; $Q_2 = Q_3 = 0.35$ ml/h; **b** $Q_1 = 0.20$ ml/h; $Q_2 = Q_3 = 0.15$ ml/h; **c** $Q_1 = 0.25$ ml/h; $Q_2 = Q_3 = 0.45$ ml/h; **d–f** $Q_1 = 0.10$ ml/h, $Q_2 = Q_3 = 0.15$ ml/h. All *scale bars* are 100 μm

spontaneously to form PLLA microspheres. Figure 4d shows the transition from liquid droplets to solid microspheres at the reservoir of 1% PVA solution using a monochrome camera attached to an IX71 inverted microscope. The region of darker color, smaller size represents solidified microspheres and droplets present with lighter color, bigger size. Figure 4e and f displays the magnified micrographs of PLLA microspheres under the microscope. Figure 5 illustrates the optical micrographs and size distribution of the produced S1-1 and S2-1 microspheres. The microspheres were uniformly spherical in shape with smooth surface. The parameters and characteristics of four microspheres in this study are shown in Table 1. The microsphere particle size was affected by the flow rate when the concentration of PLLA was fixed. In addition, TL was lower without substantially affecting the microsphere size in our experiment. Thus, the microsphere size increased slightly with the increase of TL when the concentration of PLLA was constant. The results demonstrated that the PLLA microspheres have better monodispersity than published result using the microfluidics (Lensen et al. 2010).

3.4 Drug loading, encapsulation efficiency, and in vitro release

As shown in Table 1, drug loading efficiency and the EE of PTX were quite satisfactory compared with previously published papers (Liggins and Burt 2001; Kang et al. 2008; Lu et al. 2008; Lee et al. 2008; Song et al. 2010). The TL, AL, and EE were listed in Table 1. Result indicated that the AL of four samples were 2.36 ± 0.05%, 4.64 ± 0.11%, 2.39 ± 0.02%, and 4.73 ± 0.07%, respectively. As shown in Table 1, the EE of PTX in PLLA microspheres fabricated using the microfluidics were quite satisfactory in the range of 93.95 ± 0.82% to 96.48 ± 2.31%. PTX-PLLA microspheres prepared by conventional methods usually had lower AL and EE (50–90%). The EE is an important index for DDSs, especially for an expensive drug. Compared with

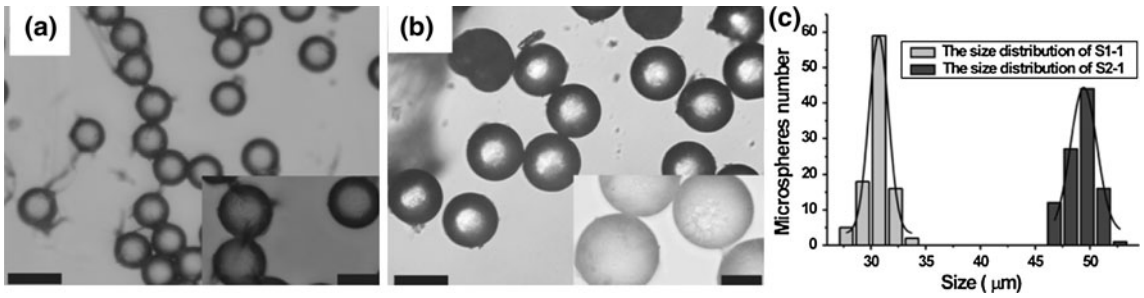

Fig. 5 Optical micrographs of PLLA microspheres with different sizes supported on cover slides. **a** S1-1 microspheres, $Q_1 = 0.15$ ml/h, $Q_2 = Q_3 = 0.35$ ml/h; **b** S2-1 microspheres, $Q_1 = 0.20$ ml/h, $Q_2 = Q_3 = 0.15$ ml/h. **c** Size distribution of the S1-1 and S2-1 microspheres (based on 100 microspheres counted by hand). The *scale bars* are 50 and 25 μm in the inserts

previously published papers (Liggins and Burt 2001; Kang et al. 2008; Lu et al. 2008; Lee et al. 2008; Song et al. 2010), the PLLA microspheres prepared by microfluidics had much higher AL and EE. The AL and EE were higher than those of previously published papers, which might not require vigorous stirring in microfluidic preparation process. In addition, it is difficult for the PTX sealed in the droplets to be diffused from the droplets. The experimental results indicate the external surface of microsphere increases with larger size, resulting in a larger attachment of PTX to external surface, a higher drug loading and a lower EE.

As one can see from Fig. 6a, the drug release follows two steps: the first is a rapid initial release of PTX within the initial 3 h (defined as burst effect) followed by a second stage where there is a gradual and sustained release. This burst effect is most likely caused by PTX molecules that were at or near the microspheres surface and escaped easily into PBS solution. Within both size ranges, initial burst exhibited a slight increase with the increase of the TL and microspheres size. It is presumed that such small initial burst was most attributed to the monodispersity of microspheres. However, the polydisperse microspheres prepared by conventional methods had a higher burst effect with more than 10% (Liggins and Burt 2001; Kang et al. 2008; Lu et al. 2008; Lee et al. 2008; Song et al. 2010). The experimental results also indicated that release ratios of the PTX decreased with the increase of PLLA microsphere size. This could be partially explained that small microspheres posses a relatively shorter diffusion pathway than those of larger size (Xu et al. 2009; Huang et al. 2009). At 720 h, 21.77, 23.57, 16.30, and 18.32% of the PTX were released, for S1-1, S1-2, S2-1, and S2-2, respectively. These results demonstrated that the PTX release from these monodisperse PLLA microspheres exhibited a very slow and sustained release for a long-term drug delivery. It also indicated that most of PTX were evenly distributed in the interior of the PLLA microspheres. The sustained release results in effective PTX concentrations at the site of pathology and may decrease systemic toxicity (Oh et al. 2008; Skwarczynski et al. 2006).

In order to understand whether the release behavior of PTX molecules from the PLLA microspheres is governed by Fickian diffusion, these results were fitted to the Higuchi model (Peppas 1985). From Fig. 6b, one can see that the logarithm of PTX cumulative amount has a linear relationship with the logarithm of release time. The values of the diffusion exponent n are less than 0.43, which indicates diffusion controlled release of the PTX through PLLA. In addition, in vitro release studies show that release of PTX from the PLLA microspheres follows Higuchi's kinetic model. The correction coefficients (R) of Higuchi's kinetic model are shown in Table 1. We presume that the influence of microsphere size on drug release followed diffusion pathway. This is in accordance to our finding that larger micropheres with longer diffusion pathway prolong the duration of drug release.

4 Conclusion

In this article, we have presented a simple surface modification method for yielding of superhydrophilic surface in PDMS microchannels. We demonstrate the fabrication of monodisperse O/W droplets and PTX-loaded PLLA microspheres of varying sizes using the modification chip. The size of droplets and microspheres can be easily controlled by regulating the flow rate. The release experiments identify a tunable and sustained release behavior of PTX from PLLA microspheres and the release process follows Fick's law. The release profiles for various drugs can be precisely characterized due to perfect monodispersity and consistency in quality of microspheres among batches. Thus, microfluidic chip method significantly improves the monodispersity of polymeric microspheres and allows for providing many potential applications for drug delivery and cell transplant in clinical treatment (Dendukuri and Doyle 2009; Skwarczynski et al. 2006; Murua et al. 2008).

Compared with conventional preparation methods, the current problem of microfluidic droplet method is of actual low throughput, so the scaling up of the productivity per

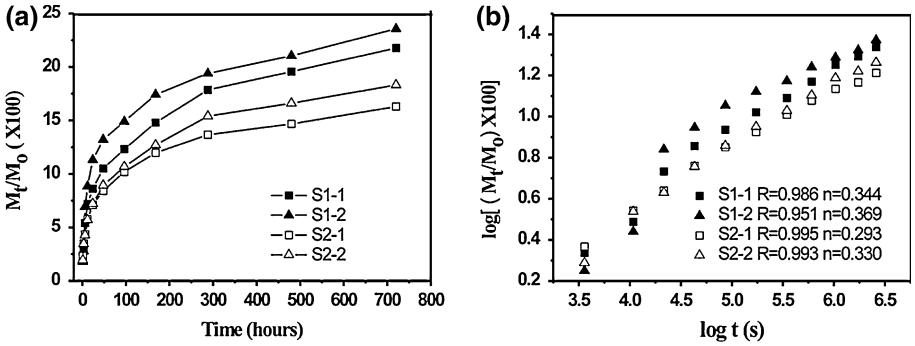

Fig. 6 Release profiles for PTX through different sizes of PTX-loaded PLLA microspheres in PBS (pH 7.4) at room temperature. **a** The cumulative release in the study time. **b** Plot $\log(M_t/M_o)$ as a function of log t

module is essential for industrial production and application. There has been recent work in developing methods to scale up droplet-based processes including parallel generation schemes and large-scale integration (Nisisako et al. 2006, Nisisako and Torri 2008). Hence, highly arrayed parallel channels based on three-dimensional structure could offer high throughput for large-scale applications. Due to the simple and cost-effective nature of the methods developed here, we believe it is possible to implement large-scale integration to efficiently improve the throughput of the microfluidic methods. The established microfluidic techniques may be adapted to microspheres fabrication of various materials in biomedical and tissue engineering.

Acknowledgments This research was supported by funding from National Basic Research Program (973 Program) of China (No. 2007CB714505), National Major Special Project of Science and Technology (No. 2009ZX09311-01) and Ministry of Education of China (No. 20080031012). The authors would like to thank Professor Zhang Xi (Tsinghua University) for measuring contact angle, ATR-FTIR and AFM images.

References

Barratt G (2003) Colloidal drug carriers: achievements and perspectives. Cell Mol Life Sci 60:21–37

Dendukuri D, Doyle PS (2009) The synthesis and assembly of polymeric microparticles using microfluidics. Adv Mater 21:1–16

Freiberg S, Zhu X (2004) Polymer microspheres for controlled drug release. Int J Pharm 282:1–18

Gong XQ, Peng SL, Wen WJ, Shen P, Li WH (2009) Design and fabrication of magnetically functionalized core/shell microspheres for smart drug delivery. Adv Funct Mater 19:292–297

Huang SH, Khoo HS, ChienChang SH, Tseng FG (2008) Synthesis of bio-functionalized copolymer particles bearing carboxyl groups via a microfluidic device. Microfluid Nanofluid 5:459–468

Huang KS, Lu K, Yeh CS, Chung SR, Lin CH, Yang CH, Dong YS (2009) Microfluidic controlling monodisperse microdroplet for 5-fluorouracil loaded genipin-gelatin microcapsules. J Control Release 137:15–19

Hung LH, The SY, Jester J, Lee AP (2010) PLGA micro/nanosphere synthesis by droplet microfluidic solvent evaporation and extraction approaches. Lab Chip 10:1820–1825

Kang YQ, Wu J, Yin GF, Huang ZB, Liao XM, Yao YD, Ouyang P, Wang HJ, Yang Q (2008) Characterization and biological evaluation of paclitaxel-loaded poly(L-lactic acid) microparticles prepared by supercritical CO_2. Langmuir 24:7432–7441

Kim DK, Dobson J (2009) Nanomedicine for targeted drug delivery. J Mater Chem 19:6294–6307

Kim J, Chaudhury MK, Owen MJ, Orbeck T (2001) The mechanisms of hydrophobic recovery of polydimethylsiloxane elastomers exposed to partial electrical discharges. J Colloid Interface Sci 244:200–207

Kim JW, Utada AS, Fernandez-Nieves A, Hu ZB, Weitz DA (2007) Fabrication of monodisperse gel shells and functional microgels in microfluidic devices. Angew Chem Int Ed 46:1819–1822

Kozlov M, Quarmyne M, Chen W, MaCarthy TJ (2003) Adsorption of poly (vinyl alcohol) onto hydrophobic substrates. A general approach for hydrophilizing and chemically activating surface. Macromolecules 36:6054–6059

Lam CNC, Kim N, Hui D, Kwok DY, Hair ML, Neumann AW (2001) The effect of liquid properties to contact angle hysteresis. Colloids Surf A 189:265–278

Lassalle V, Ferreira ML (2007) PLA nano- and microparticles for drug delivery: an overview of the methods of preparation. Macromol Biosci 7:767–783

Lee LY, Wang CH, Smith KA (2008) Supercritical antisolvent production of biodegradable micro- and nanoparticles for controlled delivery of paclitaxel. J Control Release 125:96–106

Lensen D, Breukelen KV, Vriezema DM, Hest JCMV (2010) Preparation of biodegradable liquid core PLLA microcapsules and hollow PLLA microcapsules using microfluidics. Macromol Biosci 10:475–480

Liang SM, Huang QR, Liu LS, Yam KL (2009) Microstructure and molecular interaction in glycerol plasticized chitosan/poly(vinylalcohol) blending films. Macromol Chem Phys 210:832–839

Liggins RT, Burt HM (2001) Paclitaxel loaded poly(L-lactic acid) microspheres: properties of microspheres made with low molecular weight polymers. Int J Pharm 222:19–33

Liggins RT, Burt HM (2004) Paclitaxel-loaded poly(L-lactic acid) microspheres 3: blending low and high molecular weight polymers to control morphology and drug release. Int J Pharm 282:61–71

Liggins RT, D'Amours S, Demetrick JS, Machan LS, Burt HM (2000) Paclitaxel loaded poly(L-lactic acid) microspheres for the prevention of intraperitoneal carcinomatosis after a surgical repair and tumor cell spill. Biomaterials 21:1959–1969

Lim HJ, Cho EC, Shim J, Kim DH, An EJ, Kim J (2008) Polymer-associated liposomes as a novel delivery system for cyclodextrin-bound drugs. J Colloid Interface Sci 320:460–468

Little SR, Lynn DM, Ge Q, Anderson DG, Puram SV, Chen J, Eisen HN, Langer R (2004) Poly-beta amino ester-containing microparticles enhance the activity of nonviral genetic vaccines. Proc Natl Acad Sci USA 101:9534–9539

Lu JJ, Jackson JK, Gleave ME, Burt HM (2008) The preparation and characterization of anti-VEGFR2 conjugated, paclitaxel-loaded PLLA or PLGA microspheres for the systemic targeting of human prostate tumors. Cancer Chemother Pharm 61:997–1005

Marre S, Jensen KF (2010) Synthesis of micro and nanostructures in microfluidic systems. Chem Soc Rev 39:1183–1202

Mora MF, Giacomelli CE, Garcia CD (2007) Electrophoretic effects of the adsorption of anionic surfactants to poly(dimethylsiloxane)-coated capillaries. Anal Chem 79:6675–6681

Murua A, Portero A, Orive G, Hernandez RM, Castro MD, Pedraz JL (2008) Cell microencapsulation technology: towards clinical application. J Control Release 132:76–83

Nisisako T, Torri T (2008) Microfluidic large-scale integration on a chip for mass production of monodisperse droplets and particles. Lab Chip 8:287–293

Nisisako T, Torii T, Takahashi T, Takizawa Y (2006) Synthesis of monodisperse bicolored Janus particles with electrical anisotropy using a microfluidic co-flow system. Adv Mater 18:1152–1156

Oh JK, Drumright R, Siegwart DJ, Matyjaszewski K (2008) The development of microgels/nanogels for drug delivery applications. Prog Polym Sci 33:448–477

Park JS, Lee JH, Shin HS, Lee TW, Kim MS, Khang G, Rhee JM, Lee HK, Lee HB (2007) Biodegradable polymer microspheres for controlled drug release. Tissue Eng Regen Med 4:347–359

Peppas NA (1985) Analysis of Fickian and non-Fickian drug release from polymers. Pharm Acta Helv 60:110–111

Ritger PL, Peppas NA (1987) A simple equation for description of solute release I. Fickian and non-Fickian release from non-swellable devices in the form of slabs, spheres, cylinders or discs. J Control Release 5:23–36

Shum HC, Kim JW, Weitz DA (2008) Microfluidic fabrication of monodisperse biocompatible and biodegradable polymersomes with controlled permeability. J Am Chem Soc 130:9543–9549

Skwarczynski M, Hayashi Y, Kiso Y (2006) Paclitaxel prodrugs: toward smarter delivery of anticancer agents. J Med Chem 49:7253–7269

Song TT, Yuan XB, Sun AP, Wang H, Kang CS, Ren Y, He B, Sheng J, Pu PY (2010) Preparation of injectable paclitaxel sustained release microspheres by spray drying for inhibition of glioma in vitro. J Appl Polym Sci 115:1534–1539

Spencer CM, Faulds D (1994) Paclitaxel—a review of its pharmacodynamic and pharmacokinetic properties and therapeutic potential in the treatment of cancer. Drugs 48:794–847

Suyatma NE, Tighzert L, Copinet A (2005) Effects of hydrophilic plasticizers on mechanical, thermal, and surface properties of chitosan films. J Agric Food Chem 53:3950–3957

Szebeni J, Muggia FM, Alving CR (1998) Complement activation by Cremophor EL as a possible contributor to hypersensitivity to paclitaxel: an in vitro study. J Natl Cancer Inst 90:300–306

Tan WH, Takeuchi S (2007) Monodisperse alginate hydrogel microbeads for cell encapsulation. Adv Mater 19:2696–2701

Teh SY, Lin R, Hung LH, Lee AP (2008) Droplet microfluidics. Lab Chip 8(2):198–220

Wang LY, Ma GH, Su ZG (2005) Preparation of uniform sized chitosan microspheres by membrane emulsification technique and application as a carrier of protein drug. J Control Release 106:62–75

Wei Z, Hao JG, Yuan S, Li YJ, Juan W, Sha XY, Fang XL (2009) Paclitaxel-loaded Pluronic P123/F127 mixed polymeric micelles: formulation, optimization and in vitro characterization. Int J Pharm 376:176–185

Whitesides GM (2006) The origins and the future of microfluidics. Nature 442:368–373

Wong I, Ho CM (2009) Surface molecular property modifications for poly(dimethylsiloxane) (PDMS) based microfluidic devices. Microfluid Nanofluid 7:291–306

Wu DP, Luo Y, Zhou XM, Dai ZP, Lin BC (2005) Multilayer poly(vinyl alcohol)-adsorbed coating on poly(dimethylsiloxane) microfluidic chips for biopolymer separation. Electrophoresis 26:211–218

Xia YN, Whitesides GM (1998) Soft lithography. Annu Rev Mater Sci 28:153–184

Xu S, Nie ZH, Seo M, Lewis P, Kumacheva E, Stone HA, Garstecki P, Weibel DB, Gitlin I, Whitesides GM (2005) Generation of monodisperse particles by using microfluidics: control over size, shape, and composition. Angew Chem Int Ed 44:724–728

Xu QB, Hashimoto M, Dang TT, Hoare T, Kohane DS, Whitesides GM, Langer R, Anderson DG (2009) Preparation of monodisperse biodegradable polymer microparticles using a microfluidic flow-focusing device for controlled drug delivery. Small 5:1575–1581

Yeh CH, Lin YC (2009) Using a cross-flow microfluidic chip for monodisperse UV-photopolymerized microparticles. Microfluid Nanofluid 6:277–283

Zhang K, Liang QL, Ma S, Mu X, Hu P, Wang YM, Luo GA (2009) On-chip manipulation of continuous picoliter-volume superparamagnetic droplets using a magnetic force. Lab Chip 9:2992–2999

Zhao LB, Pan L, Zhang K, Guo SS, Liu W, Wang Y, Chen Y, Zhao XZ, Chan HLW (2009) Generation of Janus alginate hydrogel particles with magnetic anisotropy for cell encapsulation. Lab Chip 9:2981–2986

Zhou JW, Ellis AV, Voelcker NH (2010) Recent developments in PDMS surface modification for microfluidic devices. Electrophoresis 31:2–16

Zhu LP, Li YG, Zhang QH, Wang HZ, Zhu MF (2010) Fabrication of monodisperse, large-sized, functional biopolymeric microspheres using a low-cost and facile microfluidic device. Biomed Microdevices 12:169–177